

Approximate Evaluation of Label-Constrained Reachability Queries

Stefania Dumbrova

ENS Rennes & CNRS IRISA & INRIA

stefania.dumbrova@inria.fr

Amaia Nazabal Ruiz Diaz

University of Lyon 1 & CNRS LIRIS

amaia.nazabal-ruiz-diaz@univ-lyon1.fr

Angela Bonifati

University of Lyon 1 & CNRS LIRIS

angela.bonifati@univ-lyon1.fr

Romain Vuillemot

Ecole Centrale Lyon & CNRS LIRIS

romain.vuillemot@ec-lyon.fr

ABSTRACT

The current surge of interest in graph-based data models mirrors the usage of increasingly complex reachability queries, as witnessed by recent analytical studies on real-world graph query logs. Despite the maturity of graph DBMS capabilities, complex label-constrained reachability queries, along with their corresponding aggregate versions, remain difficult to evaluate. In this paper, we focus on the approximate evaluation of counting label-constrained reachability queries. We offer a human-explainable solution to graph Approximate Query Processing (AQP). This consists of a summarization algorithm (GRASP), as well as of a custom visualization plug-in, which allows users to explore the obtained summaries. We prove that the problem of node group minimization, associated to the creation of GRASP summaries, is NP-complete. Nonetheless, our GRASP summaries are reasonably small in practice, even for large graph instances, and guarantee approximate graph query answering, paired with controllable error estimates. We experimentally gauge the scalability and efficiency of our GRASP algorithm, and verify the accuracy and error estimation of the graph AQP module. To the best of our knowledge, ours is the first system capable of handling visualization-driven approximate graph analytics for complex label-constrained reachability queries.

1 INTRODUCTION

A tremendous amount of information stored in graph-shaped format can be inspected, by leveraging the already mature query capabilities of graph DBMSs [5, 6, 9]. However, arbitrarily complex graph reachability queries, entailing rather intricate and possibly recursive graph patterns (required to extract friendship relationships, in social networks, or protein-to-protein interactions, in biological networks), prove difficult to evaluate, even on small-sized graph datasets [8, 26, 35]. On the other hand, the usage of these queries has radically increased in real-world graph query logs, as shown by recent empirical studies on Wikidata and DBpedia corpuses [10, 28]. For example, the percentage of SPARQL property paths has grown from 15% to 40%, for organic Wikidata queries, from 2017 to beginning 2018 [28].

In this paper, we aim to offer *human-explainable approximate graph query processing*, by focusing on regular path queries that identify graph paths, through regular expressions on edge labels. Interactive data analytics, especially addressing the relational case, has provided query result estimates with bounded errors, relying on approximate query processing (AQP) techniques [12, 30]. While many AQP systems have been proposed for diverse sets of

SQL aggregate queries, exploiting biased sampling (e.g., BlinkDB [2]) and online aggregation for the mass of value distributions (e.g., G-OLA [42]) or for rare populations (e.g., IDEA [19]), AQP for graph databases has remained unexplored so far.

We target VAGQP (Visualization-driven Approximate Graph Query Processing) for counting reachability queries that are label-constrained. The exact evaluation of these queries is #P-complete, following a result on the enumeration of simple graph paths, due to Valiant [38]. We rather focus on its *approximation* and show how it can be effectively used in practice.

Sampling approaches, customarily used for relational AQP, are not directly applicable to graph processing, due to the lack of the linearity assumption [22]¹. In view of this, we rely on a novel, query and workload-driven, graph summarization technique that provides the baseline data structure for VAGQP.

While designing VAGQP, we devoted particular attention to facilitating the exploratory steps carried out during the analytical process. We thus conceived an exploratory visualizer, capable of showing the degree of approximation of the graph summaries, for human understanding and result explanation. Consequently, we offer alternative and more compact visualizations of the envisioned graph summaries, using *linked treemaps*.

Our techniques are seamlessly designed for *property graphs*, attaching data values to property lists on both nodes and edges and, thus, keeping pace with the latest developments in graph databases and graph query languages [4, 5].

To the best of our knowledge, ours is the first work on approximate graph analytics that addresses counting estimation on top of navigational graph queries. Furthermore, we tackle both *graph visualization* and *programming APIs for graph query languages*, identified among the top 3 graph processing challenges, in a recent user survey [33]. We first provide efficient in-DBMS translations of queries formulated on an initial graph to corresponding *approximate queries*, on top of the graph's GRASP summary. We then extensively rely on exploratory data analysis to help users identify, in the linked treemap summary encoding, the regions that are relevant to the approximate query evaluation process.

We illustrate our problem through the running example below.

Example 1.1 (Graph AQP for Social Network Advertising). Let \mathcal{G}_{SN} (see Fig. 2) represent a social network, whose schema is inspired by the LDDB benchmark. Entities are people (type Person, P_i) that *know* (l_0) and/or *follow* (l_1) either each other or certain forums (type Forum, F_i). These are *moderated* (l_2) by specific persons and can *contain* (l_3) messages/ads (type Message, M_i), to which persons can *author* (l_4) other messages in *reply* (l_5). \mathcal{G}_{SN} exemplifies a graph instance adhering to the property graph

¹The linear relationship between the sample size and execution time typical of relational query processing falls apart in graph query processing.

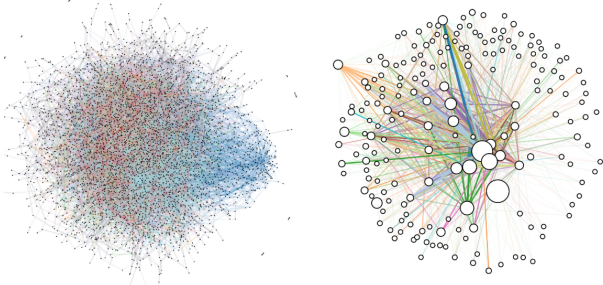


Figure 1: Original Graph (left) and Graph Summary (right) for 5K LDBC social network using node link visualization.

model (PGM) that we will define in Section 2. Our goal is to **perform graph AQP to obtain high-accuracy, fast, query estimates**. A practical application in this scenario would be leveraging AQP to obtain targeted advertising markers in social networks. To make use of the heterogeneity of real-world networks, we need to express aggregate queries in a query language allowing labeled constraints. This corresponds to a dialect of Regular Path Queries [4, 6, 40] and suffices to express the aggregate RPQ-based query types illustrated below ².

Simple and Optional Label. The count of node pairs that satisfy Q_1 , i.e., $(\) \xrightarrow{I_5} (\)$, captures the number of ad *reactions*, while the corresponding count for Q_2 , i.e., $(\) \xrightarrow{I_2^?} (\)$ indicates the number of *actual and potential moderators*.

Kleene Plus/Kleene Star. The number of the *connected acquaintances/potentially connected acquaintances* is the count of node pairs satisfying Q_3 , i.e., $(\) \xleftarrow{I_0^+} (\)$, respectively, Q_4 , i.e., $(\) \xleftarrow{I_0^*} (\)$. **Disjunction.** The number of the *targeted subscribers* is the sum of counting all node pairs satisfying Q_5 , i.e., $(\) \xleftarrow{I_4} (\)$ or $(\) \xleftarrow{I_1} (\)$.

Conjunction. The *direct reach* of a company via its page ads is the count of all node pairs satisfying Q_6 , i.e., $(\) \xleftarrow{I_4} (\) \xrightarrow{I_5} (\)$.

Conjunction with Property Filters. Recommendation systems can then further refine the Q_6 estimates by also taking into account particular properties associated to nodes. This can be done by determining the *direct demographic reach* targeting people within a certain age group, e.g., 18-24, counting all node pairs that satisfy Q_7 , i.e. $(x) \xleftarrow{I_4} (\) \xrightarrow{I_5} (\)$, where $x.age \geq 18$ and $x.age \leq 24$.

Contributions. The paper tackles the following key challenges: **Query-oriented Graph Summarization.** The direct evaluation of the above analytical queries on the original graph can be costly in terms of runtime. To address this, we design the GRASP summarization algorithm, aimed at preserving label-constrained reachability information and at book-keeping additional AQP-relevant statistics in the summary’s node properties. Unlike existing graph summarization methods for labeled graphs, based on grouping, compression or influence [27], GRASP explicitly inspects the query workload and takes into account the labels deemed as important, in order to provide a compression suitable for graph analytical applications. The produced graph summary, grouping nodes into supernodes (SN) and merging them in hypernodes (HN), is guaranteed to be encoded as a property graph, similarly to the original graph, thus allowing the evaluation of approximate queries directly in the graph database. We additionally provide

²For ease of exposition, their translation in a high-level syntax is reported in Figure 5 in Section 2.

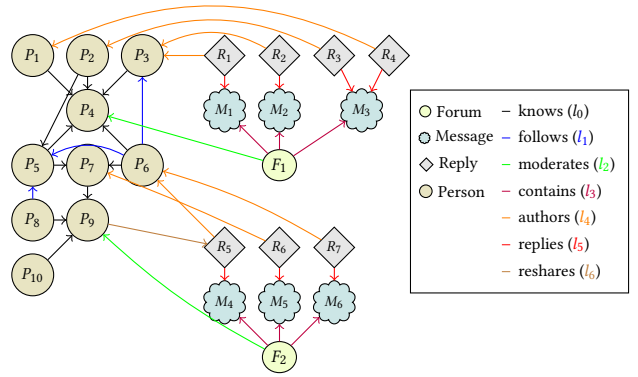


Figure 2: Example Social Graph \mathcal{G}_{SN}

an alternative visual representation of the obtained graph summary, which enables the user to understand its compactness and compression ratio (see Figure 1 right-hand-side for a grasp of the latter, on a 5K LDBC social network graph ³.)

Blending Visual and Numerical Graph AQP. The node-link representation of the graph summary, as illustrated in Figure 1, is not tailored for VAGQP. In view of this, we introduce linked treemaps, a visualization overlay, considering supernodes and hypernodes, along with their interconnecting edges in the graph summary. Inspired by previous work on semantic substrates for network exploration [7, 18], we rely on treemaps as semantic overlays for multi-labeled graphs and adapt them to our purposes. We let the user locate the densest/sparsest graph regions to be inspected by the VAGQP engine on the linked treemaps. VAGQP is coupled with an automatic translation of the queries, expressed in an RPQ dialect, into corresponding ones, in the same dialect, on the graph summary, further leveraging node properties.

Small Error Bounds and Experimental Analysis. First, we define a seamless translation, guaranteeing that queries on the summary and on the initial graph are expressible in the same fragment. Based on this, we experimentally illustrate the small relative errors of GRASP-based AQP, for each supported query type.

Our analysis also proves the effectiveness and efficiency of the GRASP algorithm on datasets with varying degrees of heterogeneity and sizes. We show that the error bounds for various query workloads, using disjunctions, single-label, Kleene-star, Kleene-plus, Optionality and Concatenations of different lengths (up to the sizes observed in practical studies), are relatively small and bearable. Apart from the high accuracy, we measure the relative response time of answering counting label-constrained reachability queries on summaries, compared to that on the original graph. For a small query subset supported by both systems, we compare with SumRDF [34], a baseline RDF graph summary, and show the better accuracy and query runtime of our approach. Finally, we show the utility of linked treemaps in restricting approximate query evaluation to specific graph regions.

The paper is organized as follows. In Section 2, we present the considered graph model and query language. In Section 3, we detail our proposed query-oriented, parametric, graph summarization algorithm (GRASP) along with its visual, linked treemap, counterpart. We explain the query translation needed for performing AQP on the summarized graph, in Section 4.1, and the

³More details about Figure 1 will be given in Section 3.3.

| | |
|----------|---|
| Edges | $e ::= \epsilon \mid \lambda l_e \cdot (p_1, t_1), \dots, (p_n, t_n), \text{ for } l_e \in L_E \cup \mathcal{V},$ $\gamma(e) = l_e, \text{ and } \sigma(l_e) = \{p_1, \dots, p_n\} \subseteq \mathcal{P}$ |
| Vertices | $v ::= x \in \mathcal{V} \mid \lambda l_v \cdot (p_1, t_1), \dots, (p_n, t_n), \text{ for } l_v \in L_V \cup \mathcal{V},$ $\gamma(v) = l_v, \text{ and } \sigma(l_v) = \{p_1, \dots, p_n\} \subseteq \mathcal{P}$ |
| Terms | $t ::= \perp \mid c \in C$ |

Figure 3: Property Graph Model

visualization techniques leveraged to identify summarization parameters, in Section 4.2. To gauge the performance of AQP on GRASP-summaries over graphs with various characteristics, we conduct an extensive experimental assessment in Section 5. We present related work in Section 6 and conclude in Section 7.

2 PRELIMINARIES

Graph Model. We take the *property graph model* (PGM) [4] as our underlying formalism (see Fig 3). Graph instances are thus multi-edge digraphs; its objects are represented by typed, data vertices and the relationships between these, as typed, labeled edges. Both vertices and edges can have any number of associated *properties* (key/value pairs); we denote the set of all properties as \mathcal{P} . Let γ_V and γ_E be disjoint vertex and edge types, whose elements we denote as L_V , resp., L_E . We call $\mathcal{G} = (V, E)$, where $E \subseteq V \times L_E \times V$, a *graph instance*, with V and E , disjoint sets of vertices v and, respectively, of edge labels l_e . Vertices v have a label id, l_v , of type L_V , and a set of property labels (attributes l_i), each with a certain, potentially undefined, respective term value t_1, \dots, t_n . We denote the vertex and edge labeling function as $\gamma : E \cup V \rightarrow L_E \cup L_V$ and the schema function, as $\sigma : L_E \cup L_V \rightarrow \mathcal{P}$. We henceforth use a binary notation for edges and, given $e \in E$, $e = l(v_1, v_2)$, we abbreviate l as $\gamma(e)$, v_1 as $e.1$ and v_2 as $e.2$. For a given edge label, l , we abbreviate its number of occurrences in \mathcal{G} as $\#l$. For a label set, $\Lambda = \{l_e^1, \dots, l_e^n\}$, its associated *frequency list* is $\vec{\Lambda} = [l_1, \dots, l_n]$, where $l_1 = l_e^{i_1}, \dots, l_n = l_e^{i_n}$ and $\{i_1, \dots, i_n\}$ is a permutation of $\{1, \dots, n\}$, such that $\#l_e^{i_1} \geq \dots \geq \#l_e^{i_n}$. For a graph $G = (V, E)$, its set of edge labels is $\Lambda(\mathcal{G}) = \{\gamma(e) \mid e \in E\}$ and, for a \mathcal{G} -subgraph, $\mathcal{G}' = (V', E')$, its set of incoming/outgoing edge labels is $\Lambda_+(\mathcal{G}') = \{\gamma(e) \mid e \in E \wedge e.2 \in V' \wedge e.1 \notin V'\}$ and $\Lambda_-(\mathcal{G}') = \{\gamma(e) \mid e \in E \wedge e.1 \in V' \wedge e.2 \notin V'\}$.

Graph Query Language. To query the above property graph model, we rely on a fragment of *regular path queries* (RPQ) ([11], [13], [14]), which we enrich with aggregate operators, as depicted in Fig. 4. RPQs correspond to property paths in SPARQL 1.1 and are a well-studied query class tailored to express *label-constrained graph reachability patterns*, consisting of one or more *label-constrained reachability paths*. Given an alphabet L_E of edge labels l_e and vertices v_1 and v_k , the *labeled path* π , corresponding to $v_1 \xrightarrow{l_e^1} v_2 \dots v_{k-1} \xrightarrow{l_e^k} v_k$, is the edge label concatenation $l_e^1 \dots l_e^k$. In their full generality, RPQs allow to select vertices connected via such labeled paths that belong to a *regular language* over L_E . To our ends, we restrict RPQs to handle *atomic paths* – bi-directional, optional, single-labeled ($l_e, l_e?$, and l_e^-) and transitive single-labeled (l_e^*) – and *composite paths* – conjunctive and disjunctive composition of atomic paths ($l_e \cdot l_e$ and $\pi + \pi$). The expressivity of the identified fragment is thus on par with that of Cypher. While not as general as SPARQL, it retains relevance, since it, for example, already captures more than 60% of the property path SPARQL queries users write in practice [10].

Moreover, this captures property path queries, as found in both the Wikidata online query collection and the Wikidata large

| | |
|---------|---|
| Clauses | $C ::= A \leftarrow A_1, \dots, A_n \mid Q \leftarrow A_1, \dots, A_n$ |
| Queries | $Q ::= \text{Ans}(p_1, \dots, p_m, \text{count}(x_1, \dots, x_n))$ |
| Atoms | $A ::= \pi(l_{v_1}, l_{v_2}), \text{ for } l_{v_1}, l_{v_2} \in L_V \mid \leq(l_{v_1}, l_{v_2}) \mid$ $<(l_{v_1}, l_{v_2}) \mid \geq(l_{v_1}, l_{v_2}) \mid >(l_{v_1}, l_{v_2})$ |
| Paths | $\pi ::= \epsilon \mid l_e \mid l_e? \mid l_e^{-1} \mid l_e^*, \text{ for } l_e \in L_E \mid \pi + \pi \mid l_e \cdot l_e$ |

Figure 4: Graph Query Language

| | |
|-----------------|--|
| $Q_1(l_5)$ | $\text{Ans}(\text{count}(_)) \leftarrow l_5(_, _)$ |
| $Q_2(l_2)$ | $\text{Ans}(\text{count}(_)) \leftarrow l_2^*(_, _)$ |
| $Q_3(l_0)$ | $\text{Ans}(\text{count}(_)) \leftarrow l_0^+(_, _)$ |
| $Q_4(l_0)$ | $\text{Ans}(\text{count}(_)) \leftarrow l_0^-(_, _)$ |
| $Q_5(l_4, l_1)$ | $\text{Ans}(\text{count}(_)) \leftarrow l_4 + l_1(_, _)$ |
| $Q_6(l_4, l_5)$ | $\text{Ans}(\text{count}(_)) \leftarrow l_4 \cdot l_5(_, _)$ |
| $Q_7(l_4, l_5)$ | $\text{Ans}(\text{count}(x)) \leftarrow l_4 \cdot l_5, \geq(x.\text{age}, 18), \leq(x.\text{age}, 24)$ |

Figure 5: Targeted Advertising Marker Queries

corpus studied in [28]. These are further enriched with the *count* operator, to support basic graph reachability estimates.

Example 2.1. We report in Figure 5 the queries of Example 1.1 expressed by using the syntax of Figure 4.

3 GRAPH SUMMARIZATION

Let us assume a graph $\mathcal{G} = (V, E)$ and a edge label set $\Lambda_Q \subseteq \Lambda(\mathcal{G})$. We introduce the *GRASP summarization* algorithm, which compresses \mathcal{G} into an AQP-amenable property graph, $\hat{\mathcal{G}}$, tailored for counting label-constrained reachability queries (see Fig. 4), whose labels are all in Λ_Q . Note that we place ourselves in the *static* setting, as GRASP relies on transitive closure computation, whose maintenance under updates constitutes an orthogonal problem to the one we target, as originally identified in [31].

The GRASP summarization, described in Algorithm 1, consists of three phases. The **grouping phase** computes Φ , a label-driven partitioning of \mathcal{G} into *groupings*, following the label-connectivity on the most frequently occurring edge labels in $\Lambda(\mathcal{G})$. Next, the **evaluation phase** refines the previous step, by further isolating into *supernodes* the grouping components that satisfy a custom property concerning label-connectivity. The **merge phase** then fuses supernodes into *hypernodes*, based on label-reachability similarity conditions, as specified by each heuristic mode m .

Algorithm 1 GRASP($\mathcal{G}, \Lambda_Q, m$)

Input: \mathcal{G} – a graph; $\Lambda_Q \subseteq \Lambda(\mathcal{G})$ – a set of query labels;
 m – heuristic mode boolean switch

Output: $\hat{\mathcal{G}}$ – a graph summary

- 1: $\Phi \leftarrow \text{GROUPING}(\mathcal{G})$
- 2: $\mathcal{G}^* \leftarrow \text{EVALUATION}(\Phi, \Lambda_Q)$
- 3: $\hat{\mathcal{G}} \leftarrow \text{MERGE}(\mathcal{G}^*, \Lambda_Q, m)$
- 4: **return** $\hat{\mathcal{G}} = (\hat{V}, \hat{E})$

The GRASP summarization phases are detailed in Sections 3.1, 3.2, and 3.3. To gauge the topological differences between realistic graph instances and their respective GRASP-summaries, we resort to visualization techniques in Section 3.4.

3.1 Grouping Phase

The **grouping phase** aims to output a partitioning Φ of \mathcal{G} , such that $|\Phi|$ is *minimized* and, for each $\mathcal{G}_i \in \Phi$, the number of occurrences of the most frequent edge label in $\Lambda(\mathcal{G}_i)$, $\max_{l \in \Lambda(\mathcal{G}_i)} (\#l)$,

is *maximized*. To this end, we first sort the set of edge labels in \mathcal{G} , $\Lambda(\mathcal{G})$, into a *frequency list*, $\overrightarrow{\Lambda(\mathcal{G})}$. Next, for each $l_i \in \overrightarrow{\Lambda(\mathcal{G})}$, in descending frequency order, we set to identify the largest subgraphs of \mathcal{G} that are weakly-connected on l_i . By relying on a *most-frequently-occurring-label* heuristic, we thus bias the graph partitioning towards a coarser-level of granularity.

The key notion required to define Φ is that of *maximal weak label-connectivity*, introduced below. Let us first introduce needed preliminary notions. In the following, we denote by $\overline{\mathcal{G}} = (V, \overline{E})$, where $|E| = |\overline{E}|$, the transformation of \mathcal{G} into an undirected graph. Also, a graph \mathcal{G}' is a *subgraph* of \mathcal{G} iff $V' \subseteq V$ and $E' \subseteq E$.

Definition 3.1 (Weak Connectivity). \mathcal{G} is *weakly connected* iff $\overline{\mathcal{G}}$ is *connected*, i.e., a path exists between any pair of V vertices.

Definition 3.2 (Maximal Weak Connectivity). A subgraph of \mathcal{G} , $\mathcal{G}' = (V', E')$ is *maximal weakly connected* iff: 1) \mathcal{G}' is weakly connected and 2) no E edge connects any V' node to $V \setminus V'$.

As we are interested in compressing \mathcal{G} by label-connectivity, we strengthen the definition of weak-connectivity below.

Definition 3.3 (Weak Label-Connectivity). Given a graph $\mathcal{G} = (V, E)$ and a label $l \in \Lambda(\mathcal{G})$, \mathcal{G} is *weakly label-connected* on l iff: 1) when converting all edges in E into undirected ones, the resulting graph, $\overline{\mathcal{G}} = (V, \overline{E})$, where $|E| = |\overline{E}|$, is *connected* and 2) when removing any l -labeled edge from \overline{E} , there exist vertices v_1, v_2 in V that are not connected in $\overline{\mathcal{G}}$ by a l^+ -labeled path.

Since we aim to capture as many vertices in each *weakly label-connected* subgraph of \mathcal{G} , we further enforce on the latter the notion of *maximality*, as defined next.

Definition 3.4 (Maximal Weak Label-Connectivity). Given a graph $\mathcal{G} = (V, E)$ and a label $l \in \Lambda(\mathcal{G})$, a subgraph of \mathcal{G} , $\mathcal{G}' = (V', E')$, is *maximal weakly label-connected* on l , denoted as $\lambda(\mathcal{G}') = l$, iff: 1) \mathcal{G}' is *weakly label-connected* on l and 2) no edge in E , with label l , connects any of the nodes in V' to $V \setminus V'$.

We outline the **grouping phase**, as captured in Algorithm 2.

Algorithm 2 GROUPING(\mathcal{G})

Input: \mathcal{G} – a graph

Output: Φ – a graph partitioning

```

  ▶ Initialization
1:  $n \leftarrow |\Lambda(\mathcal{G})|$ ,  $\overrightarrow{\Lambda(\mathcal{G})} \leftarrow [l_1, \dots, l_n]$ ,  $\Phi \leftarrow \emptyset$ ,  $i \leftarrow 1$ 
  ▶ Label-driven partitioning computation
2: for all  $l \in \overrightarrow{\Lambda(\mathcal{G})}$  do
3:    $\mathcal{G}_i \leftarrow \{\mathcal{G}_i^k = (V_i^k, E_i^k) \subseteq \mathcal{G} \mid \lambda(\mathcal{G}_i^k) = l\}$ 
4:    $\Phi \leftarrow \Phi \cup \{\mathcal{G}_i\}$ 
5:    $V \leftarrow V \setminus \bigcup_{\mathcal{G}_i^k \in \mathcal{G}_i} \{v \in V \mid v \in V_i^k\}$ 
6:    $i \leftarrow i + 1$ 
7:    $V(\Phi) \leftarrow \bigcup_{\mathcal{G}_i \in \Phi} \bigcup_{\mathcal{G}_i^k \in \mathcal{G}_i} \{v \in V \mid v \in V_i^k\}$ 
8:    $\Phi \leftarrow \Phi \cup \{\mathcal{G}_i = (V_i, E_i) \subseteq \mathcal{G} \mid V_i = V \setminus V(\Phi)\}$ 
9: return  $\Phi$ 

```

We henceforth denote $\Phi = \text{GROUPING}(\mathcal{G})$ and name each \mathcal{G}' , $\mathcal{G}' \in \Phi$, a \mathcal{G} -*grouping* and each \mathcal{G}'' , $\mathcal{G}'' \in \mathcal{G}'$, a \mathcal{G}' -*subgrouping*. Note that Φ is not unique, as, for $l_1, l_2 \in \Lambda(\mathcal{G})$, such that $\#l_1 = \#l_2$, we arbitrarily order l_1 and l_2 in $\overrightarrow{\Lambda(\mathcal{G})}$.

Definition 3.5 (Non-Trivial (Sub)Groupings). A \mathcal{G} -grouping, \mathcal{G}' , $\mathcal{G}' = (V', E')$, is called *trivial*, if $\mathcal{G}' = \mathcal{G}$ or $E' = \emptyset$, and *non-trivial*, otherwise. A \mathcal{G}' -subgrouping, $\mathcal{G}'' = (V'', E'')$, is called *trivial*, if $E'' = \emptyset$, and *non-trivial*, otherwise.

LEMMA 3.6 (NON-TRIVIAL GROUPING PROPERTIES). *Let \mathcal{G}' be a non-trivial \mathcal{G} -grouping. The following hold. P1: For any non-trivial \mathcal{G}' -subgrouping, \mathcal{G}'' , there exists $l'', l' \in \Lambda(\mathcal{G}')$, such that $\lambda(\mathcal{G}') = l'$. P2: For any non-trivial distinct \mathcal{G}' -subgroupings, $\mathcal{G}_1'', \mathcal{G}_2''$: a) $\lambda(\mathcal{G}_1'') = \lambda(\mathcal{G}_2'')$ and b) \mathcal{G}_1'' and \mathcal{G}_2'' are edge-wise disjoint.*

PROOF. P1 is provable by contradiction. If $\nexists l'', l' \in \Lambda(\mathcal{G}')$, such that $\lambda(\mathcal{G}') = l'$, then $E' = \emptyset$, contradicting the non-triviality of \mathcal{G}' . P2.a) holds by construction and P2.b), by contradiction. Assume $\mathcal{G}_1'' \cap \mathcal{G}_2'' \neq \emptyset$; then, \mathcal{G}_1'' and \mathcal{G}_2'' share at least a node, which is impossible by construction. \square

Next, let us characterize the *GROUPING* algorithm. We start with the following observations.

LEMMA 3.7 (SUBGROUPING MAXIMAL LABEL-CONNECTIVITY). *For each \mathcal{G}_i , $\mathcal{G}_i \in \Phi$, each of its maximally weakly connected components, \mathcal{G}_i^k , $\mathcal{G}_i^k \in \mathcal{G}_i$ is also maximally label-connected on l , where $\#l = \max_{l \in \Lambda(\mathcal{G}_i)} (\#l)$.*

PROOF. By construction, we know that, if $\mathcal{G}_i^k \in \mathcal{G}_i$, then there exists a label $l', l' \in \Lambda(\mathcal{G})$, such that $\lambda(\mathcal{G}_i^k) = l'$. Assume that $l' \neq l$. By definition, there exists at least one edge in E_i^k labeled l' . Since \mathcal{G}_i^k is maximally weakly label-connected on l' , then each such edge has to connect vertices that are also connected by an edge labeled l' . As $\#l \geq \#l'$, then there exists at least one pair of vertices in V_i^k that are connected by more edges labeled l than l' . Hence, $\lambda(\mathcal{G}_i^k) = l$, contradicting the hypothesis. \square

THEOREM 3.8 (GROUPING PROPERTIES). *If $|V| \geq 1$, then:*

P1: $\forall \mathcal{G}_i \in \Phi, V_i \neq \emptyset$

P2: $\forall \mathcal{G}_i, \mathcal{G}_j \in \Phi$, where $i \neq j$, $\mathcal{G}_i \cap \mathcal{G}_j = \emptyset$

P3: $\bigcup_{i \in [1, k]} V_i = V$ and $\bigcup_{i \in [1, k]} E_i \subseteq E$

P4: $\Phi = \{\mathcal{G}_i = (V_i, E_i) \subseteq \mathcal{G} \mid i \in [1, |\Lambda(\mathcal{G})| + 1]\}$

PROOF. P1, P2, P3 trivially hold. Let us prove P4. If $E = \emptyset$, $\Phi = \{\mathcal{G}\}$. Otherwise, a label $l \in \overrightarrow{\Lambda(\mathcal{G})}$ exist and we can construct a grouping \mathcal{G}_i , $\lambda(\mathcal{G}_i) = l$. Assume $\Phi > |\Lambda(\mathcal{G})| + 1$. At least two groupings, $\mathcal{G}_i, \mathcal{G}_j$, with the same most frequently occurring label, l , exist in Φ . As $|\mathcal{G}_i| \geq 1$ and $|\mathcal{G}_j| \geq 1$, each contains a maximally weakly connected component, $\mathcal{G}_i^{k_i}, \mathcal{G}_j^{k_j}$. From Lemma 3.7, $\lambda(\mathcal{G}_i^{k_i}) = \lambda(\mathcal{G}_j^{k_j})$, contradicting $\mathcal{G}_i \cap \mathcal{G}_j \neq \emptyset$. \square

We illustrate the above algorithm, in Figure 6, as follows.

Example 3.9 (Graph Grouping). Let \mathcal{G} be the graph from Figure 2. It holds that: $\#l_0 = 11$, $\#l_1 = 3$, $\#l_2 = 2$, $\#l_3 = 6$, $\#l_4 = 7$, $\#l_5 = 7$, $\#l_6 = 1$. Hence, we can take $\overrightarrow{\Lambda(\mathcal{G})} = [l_0, l_5, l_4, l_3, l_1, l_2, l_6]$. Note that, as $\#l_4 = \#l_5$, we can choose an arbitrary order between the labels in $\overrightarrow{\Lambda(\mathcal{G})}$. Following Algorithm 2, we first add \mathcal{G}_1 to Φ , as it regroups the maximal weakly-label components on l_0 . We then have $V = \{R_1, \dots, R_7, M_1, \dots, M_6, F_1, F_2\}$. Next, we add \mathcal{G}_2 to Φ , as it regroups the maximally weakly-label component on l_5 . We obtain $V = \{F_1, F_2\}$. We add the remaining subgraph, \mathcal{G}_3 , to Φ and output $\Phi = \{\mathcal{G}_1, \mathcal{G}_2, \mathcal{G}_3\}$, as illustrated in Figure 6.

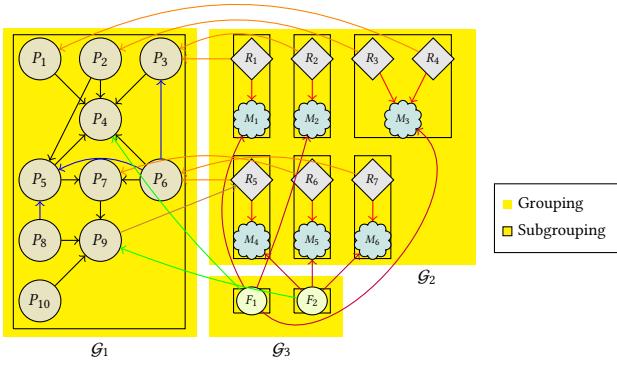


Figure 6: Summarizing \mathcal{G}_{SN} (Grouping Phase)

3.2 Evaluation Phase

The **evaluation phase** takes as input Φ , the \mathcal{G} -partitioning from Algorithm 2, and Λ_Q , a set of labels, and outputs $\mathcal{G}^* = (V^*, E^*)$, an AQP-amenable compression of \mathcal{G} . The phase creates V^* , the set of *supernodes* (SN), and E^* , the set of *superedges* (SE). After each step, \mathcal{G}^* is enriched with AQP-relevant properties, exploited in Section 4. Next, we explain how supernodes, AQP-properties, and superedges are computed.

Definition 3.10 (Supernodes (SN)). Let Φ be a \mathcal{G} -partitioning into groupings, \mathcal{G}_i . Φ is transformed into a set of supernodes, $V^* = VFUSE(\Phi)$ (see Algorithm 4). Each *supernode*, $v^* \in V^*$, is obtained by fusing all vertices and edges of each subgrouping \mathcal{G}_i^k , $\mathcal{G}_i^k \in \mathcal{G}_i$. We denote the label l , such that $\lambda(\mathcal{G}_i^k) = l$, as $\lambda(v^*)$.

Algorithm 4

Input: Φ – a graph partitioning;
Output: V^* – set of *supernodes*

- 1: $V^* \leftarrow \emptyset$
 - 2: **for all** $\mathcal{G}_i \in \Phi$ **do**
 - 3: **for all** $\mathcal{G}_i^k \in \mathcal{G}_i$ **do**
 - 4: $v_i^k \leftarrow \mathcal{G}_i^k$
 - 5: $V^* \leftarrow V^* \cup \{v_i^k\}$
 - 6: **return** V^*
-

AQP-properties. Consider $l \in \Lambda(\mathcal{G})$ and supernodes $v_i^*, v_j^* \in V^*$. We call a l -labeled edge from v_i^* to v_j^* a *cross-edge* and define $E_{i,j}(l) = \{e \in E | e.1 \in v_i^* \wedge e.2 \in v_j^* \wedge \gamma(e) = l\}$. For every $v^* \in \mathcal{G}_i^k$, we then associate $\sigma(v^*)$, a set consisting of properties that regard *compression*, *label-connectivity*, and *pairwise label-traversal*. We explain each of these below.

Compression. We record the number of *inner vertices* in v^* as $VWeight(v^*) : |V_i^k|$ and that of *inner edges* as $EWeight(v^*) : |E_i^k|$.
Label-Connectivity. The percentage-wise occurrence of l in v^* is $LPercent(v^*, l) : \frac{|\{e \in E_i^k | \gamma(e) = l\}|}{EWeight(v^*)}$. The number of vertex pairs connected with an l -labeled edge is $LReach(v^*, l) : |\{(v_1, v_2) \in V_i^k \times V_i^k | l^+(v_1, v_2) \in \mathcal{G}_i^k\}|$.

Pairwise Label-Traversal. Consider labels $l_1, l_2 \in \Lambda(\mathcal{G})$ and direction indices, $d_1, d_2 \in \{1, 2\}$. We compute the number of paths between two cross-edges with labels l_1, l_2 , directions d_1, d_2 , and a common node, as $EReach(v^*, l_1, l_2, d_1, d_2) = |\{(e_1^*, e_2^*) | \{e_1^*, e_2^*\} \subseteq$

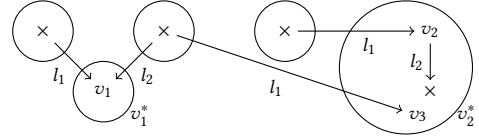


Figure 7: Traversal Nodes/Edges and Frontier Vertices

$E^* \setminus E_i^k \wedge \gamma(e_1^*) = l_1 \wedge \gamma(e_2^*) = l_2 \wedge e_1^*.d_1 = v^* = e_2^*.d_2\}$. We compute the number of *traversal edges*, i.e., inner/cross-edge pairs, e_1, e_2 , with labels l_1, l_2 , directions d_1, d_2 , and v^* as common endpoint, as $\delta(v^*, l_1, l_2, d_1, d_2) = |\{(e_1, e_2) | e_1 \in E^* \setminus E_i^k \wedge \gamma(e_1) = l_1 \wedge e_2 \in E_i^k \wedge \gamma(e_2) = l_2 \wedge e_1.d_1 = v^* = e_2.d_2\}|$. We take the number of *frontier vertices*, given a fixed label l and direction d , to be $V_F(v^*, l, d) = \{v | v \in v^* \wedge \exists e, e \in E \setminus E_i^k \wedge \gamma(e) = l \wedge e.d = v\}$. Finally, we consider the number of l_1 -labeled cross-edges relative to that of frontier vertices on l_2 to represent the *relative label participation*, computed as $RLPart(v^*, l_1, l_2, d_1, d_2) : (\sum_{v \in V_i^k} \delta(v, l_1, d_1, d_2, V \setminus V_i^k)) / |V_F(v^*, l_2, d_2)|$.

Algorithm 5 VProperties(Φ, Λ)

Input: V – a set of vertices, Λ – a set of labels;
Output: V – property-enriched set of vertices

- 1: **for all** $v \in V$ **do**
 - 2: $v.vweight \leftarrow VWeight(v)$,
 - 3: $v.eweight \leftarrow EWeight(v)$
 - 4: **for all** $(l_1, l_2) \in \Lambda, (d_1, d_2) \in \{1, 2\}$ **do**
 - 5: $v.plabel(l_1) \leftarrow LPercent(v, l_1)$
 - 6: $v.lreach(l_1) \leftarrow LReach(v, l_1)$
 - 7: $v.ereach(l_1, d_1, d_2) \leftarrow EReach(v, l_1, d_1, d_2)$
 - 8: $v.rlpert(l_1, l_2, d_1, d_2) \leftarrow RLReach(v, l_1, l_2, d_1, d_2)$
 - 9: **return** V
-

We illustrate these properties via an example.

Example 3.11 (Supernode Properties). In Fig.7, we have that $EReach(v_1^*, l_1, l_2, 1, 1) = \delta(v_2^*, l_1, l_2, 1, 2) = 1, V_F(v_2^*, l_1, 1) = \{v_1, v_3\}$.

We now proceed to explaining the creation of superedges.

Definition 3.12 (Superedges (SE)). A *superedge*, $e^* \in E^*$, is obtained by merging all cross-edges $e, e \in E_{i,j}(l), l \in \Lambda(\mathcal{G})$, as described in the below algorithm. To each such e^* we then associate a weight, $EWeight(e^*) : |\{e \in E | e \in e^*\}|$.

Algorithm 6 EFUSE(V^*, Λ)

Input: Φ – a graph partitioning, Λ_Q – a set of label pairs;
Output: \mathcal{G}^* – a graph with *supernodes* and *superedges*

- 1: $E^* \leftarrow \emptyset$
 - 2: **for all** $l \in \Lambda$ **do**
 - 3: $E_l \leftarrow \{e \in E | \gamma(e) = l\}$
 - 4: **for all** $v_i^*, v_j^* \in V^*$ **do**
 - 5: **for all** $v_i \in v_i^*, v_j \in v_j^*$ **do**
 - 6: $e^* \leftarrow \{l(v_i^*, v_j^*) | l(v_i, v_j) \in E_l\}$
 - 7: $E^* \leftarrow E^* \cup \{e^*\}$
 - 8: **return** E^*
-

The **evaluation phase** is summarized next.

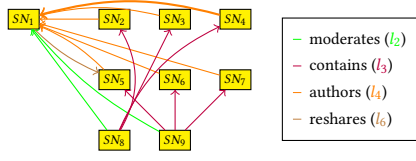


Figure 8: Summarizing \mathcal{G}_{SN} (Evaluation Phase)

Algorithm 7 EVALUATE(Φ, Λ)

Input: Φ – a graph partitioning, Λ – a set of labels;
Output: \mathcal{G}^* – a graph with *supernodes* and *superedges*

- 1: $V^* \leftarrow VFUSE(\Phi)$
 - 2: $V^* \leftarrow VProperties(V^*, \Lambda)$
 - 3: $\hat{E} \leftarrow EFUSE(V^*, \Lambda)$
 - 4: **for all** $e^* \in E^*$ **do**
 - 5: $e^*.weight \leftarrow EWeight(e^*)$
 - 6: **return** $\mathcal{G}^* = (V^*, E^*)$
-

We illustrate the above by revisiting our running example.

Example 3.13 (Graph Compression). In Figure 8, we display the supergraph \mathcal{G}^* , obtained from Φ , after the **evaluation phase**. Each supernode corresponds to a Φ -subgrouping, as depicted in Figure 6. Each superedge is obtained by compressing similarly labeled edges, whose source and, respectively, target vertices are in the same supernode. Each superedge e^* has $EWeight(e^*) = 1$, except that connecting SN_4 and SN_1 , whose edge weight is 2.

3.3 Merge Phase

The **merge phase** takes as input a graph, \mathcal{G}^* , as computed by Algorithm 9, along with a set of labels, Λ_Q , and outputs a compressed graph, $\hat{\mathcal{G}} = (\hat{V}, \hat{E})$. The phase proceeds in two steps, corresponding to the creation of \hat{V} , the set of *hypernodes* (HN), and, respectively, to that of \hat{E} , the set of *hyperedges* (HE). At each step, $\hat{\mathcal{G}}$ is enriched with *AQP-relevant properties* (see Section 4).

Hypernodes are computed by merging together supernodes based on various criteria, according to Definition 3.15. The primary, *inner-merge*, condition for merging candidate supernodes is for them to be maximal weakly label-connected on the same label. The *source-merge* heuristic additionally requires that they share the same set of outgoing labels, while the *target-merge* heuristic requires that they share the same set of ingoing labels.

Definition 3.14 (Hypernodes (HN)). Let V^* be a supernode set, where $V^* = \{v_1^*, \dots, v_n^*\}$. V^* is transformed into a set of hypernodes, $\hat{V} = VMERGE(V^*)$, where $\hat{V} = \{\hat{v}_1, \dots, \hat{v}_m\}$. A *hypernode* $\hat{v}_k \in \hat{V}$ corresponds to fusing a subset V_k^* of V^* , such that, for all $i, j \in [1, n]$, $\{v_i^*, v_j^*\} \in V_k^*$, if $\lambda(v_i^*) = \lambda(v_j^*)$, and either of the following holds: **Case 1.** $\Lambda_+(v_i^*) = \Lambda_+(v_j^*)$, for all $i, j \in [1, n]$. **Case 2.** $\Lambda_-(v_i^*) = \Lambda_-(v_j^*)$, for all $i, j \in [1, n]$. The first condition defines the *target-merge* heuristic, while the latter, the *source-merge* one.

To each such hypernode, \hat{v} , we associate a property set.

Definition 3.15 (Hypernode Properties). The *property set* of \hat{v} , $\sigma(\hat{v})$ is the same as in Definition 3.10. Except for LPercent, the values of hypernode properties are obtained by adding all those corresponding to *supernodes* v^* , such that $v^* \in \hat{v}$. For the label percentage property on a given label l , we have: $LPercent(\hat{v}, l) :$

$$\frac{\sum_{v^* \in \hat{v}} LPercent(v^*, l) * EWeight(v^*)}{\sum_{v^* \in \hat{v}} EWeight(v^*)}.$$

Superedges are merged into *hyperedges*, if they share the same label and endpoints, as defined below.

Algorithm 9

Input: V^* – a set of supernodes; Λ – a set of labels;
 m – heuristic mode

Output: \hat{V} – a set of hypernodes

- 1: **for all** $v^* \in V^*$ **do**
 - 2: $\Lambda_+(v^*) \leftarrow \{l \in \Lambda \mid \exists v_s^*, v_t^* \in V^* \wedge l(v_s^*, v_t^*) \in E^*\}$
 - 3: $\Lambda_-(v^*) \leftarrow \{l \in \Lambda \mid \exists v_t^*, v_s^* \in V^* \wedge l(v_s^*, v_t^*) \in E^*\}$
 - 4: **for all** $v_1^*, v_2^* \in V^*$ **do**
 - 5: $b_\lambda \leftarrow \lambda(v_1^*) = \lambda(v_2^*)$ ▷ *Inner-Merge Condition*
 - 6: $b_+ \leftarrow \Lambda_+(v_1^*) = \Lambda_+(v_2^*), b_- \leftarrow \Lambda_-(v_1^*) = \Lambda_-(v_2^*)$
 - 7: **if** $m = \text{true}$ **then**
 - 8: $\hat{v} \leftarrow \{v_1^*, v_2^* \mid b_\lambda \wedge b_+ = \text{true}\}$ ▷ *Target-Merge*
 - 9: **else**
 - 10: $\hat{v} \leftarrow \{v_1^*, v_2^* \mid b_\lambda \wedge b_- = \text{true}\}$ ▷ *Source-Merge*
 - 11: $\hat{V} \leftarrow \{\hat{v}_k \mid k \in [1, |\hat{V}|]\}$
 - 12: **return** \hat{V}
-

Definition 3.16 (Hyperedges (HE)). Let E^* be a superedge set, $E^* = \{e_1^*, \dots, e_n^*\}$. E^* is transformed into a hyperedge set, $\hat{E} = EMERGE(E^*)$, where $\hat{E} = \{\hat{e}_1, \dots, \hat{e}_m\}$. A *hyperedge*, \hat{e}_k , $\hat{e}_k \in \hat{E}$, corresponds to fusing a subset E_k^* of E^* , such that, for $l \in \Lambda(\mathcal{G})$ and $i, j \in [1, n]$, $\{e_i^*, e_j^*\} \subseteq E_k^*$, if $e_i^* \stackrel{l}{=} e_j^*$, $e_i^*.1 = e_j^*.1$, and $e_i^*.2 = e_j^*.2$. To each hyperedge \hat{e} we associate a weight, $EWeight(\hat{e})$, corresponding to $|E_k^*|$, the number of superedges \hat{e}_k compressed.

The **merge phase** is captured in Algorithm 11.

Algorithm 11

Input: \mathcal{G}^* – a graph; Λ_Q – a set of label pairs;
 m – heuristic mode

Output: $\hat{\mathcal{G}}$ – a graph summary

- 1: $\hat{V} \leftarrow VMERGE(V^*, \Lambda, m)$
 - 2: $\hat{V} \leftarrow VProperties(\hat{V}, \Lambda)$
 - 3: $\hat{E} \leftarrow EFUSE(E^*, \Lambda(\mathcal{G}^*))$
 - 4: **for all** $\hat{e} \in \hat{E}$ **do**
 - 5: $\hat{e}.weight \leftarrow EWeight(\hat{e})$
 - 6: **return** $\hat{\mathcal{G}} = (\hat{V}, \hat{E})$
-

Finally, we depict the resulting GRASP-summarization of our running example, as follows .

Example 3.17 (Graph Compression). The graphs in Figure 9 are obtained from $\mathcal{G}^* = (V^*, E^*)$, after the **merge phase**. Each hypernode corresponds to the fusion of the supernodes in Figure 8, by the heuristics target-merge (left) and source-merge (right).

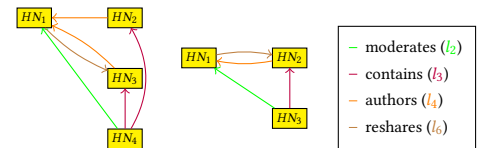


Figure 9: Summarizing \mathcal{G}_{SN} (Merge Phase)

Finally, we show the intractability of the graph summarization problem, under the conditions of our algorithm.

Definition 3.18 (Summarization Function). Let $\mathcal{G} = (V, E)$ be a graph and $\Phi = \{\mathcal{G}_i = (V_i, E_i) \mid i \in [1, |\Phi|]\}$, a \mathcal{G} -partitioning into HNs. Each HN, \mathcal{G}_i , contains HN-subgraphs, \mathcal{G}_i^k , all *maximal weakly label-connected* on a label $l \in \Lambda(\mathcal{G})$. A *summarization function* $\chi_\Lambda : V \rightarrow \mathbb{N}$ is a function assigning to each vertex, v , a unique HN identifier $\chi_\Lambda(v) \in [1, k]$. χ_Λ is *valid* if for any v_1, v_2 , where $\chi_\Lambda(v_1) = \chi_\Lambda(v_2)$, either v_1, v_2 belong to :

Case 1 the same HN-subgraph, \mathcal{G}_i^k , that is maximal weak label-connected on l , or to

Case 2 different HN-subgraphs, $\mathcal{G}_i^{k_1}, \mathcal{G}_i^{k_2}$, each maximal label-connected on l and not connected by an l -labeled edge in \mathcal{G} .

THEOREM 3.19 (OPTIMAL SUMMARIZATION NP-COMPLETENESS).

Let **MinSummary** be the problem that, given a graph \mathcal{G} and an integer $k' \geq 2$, decides whether there exists a label-driven partitioning Φ of \mathcal{G} with $|\Phi| \leq k'$, such that χ_Λ is a valid summarization. Then, **MinSummary** is NP-complete, even for undirected graphs, $|\Lambda(\mathcal{G})| \leq 2$ and $k' = 2$.

PROOF. We establish the result in two steps.

MinSummary is in NP. We construct a valid *summarization function*, χ_Λ , as a witness. For a graph partitioning in k subgraphs, one can verify in polynomial time (see [24]) if two vertices are reachable by a given labeled-constrained path and decide if their assignment to the same or to different HNs is valid (Def. 3.18).

MinSummary is NP-hard. Let us henceforth reduce the **MinSummary** problem to **IndSet**, i.e., the NP-complete (see [20]) problem of establishing whether an undirected graph contains K independent vertices, for an arbitrary K . We prove **IndSet** \leq_p **MinSummary**. Let $\mathcal{G} = (V, E)$ be an **IndSet** instance, where \mathcal{G} is undirected, $|V| = n \geq 2$, $|E| = m$, $\Lambda(\mathcal{G}) = \{l_1\}$. We consider a polynomial reduction function, f , such that $f(\mathcal{G}) = \mathcal{G}'$, $\mathcal{G}' = (V', E')$ (see Fig. 10), $\{v'_1, v'_2, v'_3\} \subset V'$, $\Lambda(\mathcal{G}') = \{l_1, l_2\}$, and $\tilde{\mathcal{G}} \subset \mathcal{G}'$, where $\tilde{\mathcal{G}}$ is obtained from \mathcal{G}' , by adding, between each pair of vertices connected with an l_1 -labeled edge, n more l_1 -labeled edges. Let \mathcal{G}' contain three paths of length k , between v'_1 and v'_2 (one, l_1 -labeled, and two, l_2 -labeled) and two paths of length n , between v'_2 and v'_3 , of each color. Let $K \geq 0$ be the number of independent vertices in \mathcal{G} . In \mathcal{G}' , $\#l_1 \geq (n+1)(n-K-1) + 2k + n$ and $\#l_2 = 2n + k$. $l_2 = \max_{l \in \mathcal{G}'}(\#l) \Rightarrow K \geq \frac{n^2 - n - 1 + k}{n + 1} \geq 1$.

We show: \mathcal{G} satisfies **IndSet** $\Leftrightarrow \mathcal{G}'$ satisfies **MinSummary**.

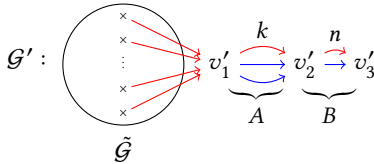


Figure 10: \mathcal{G}' Construction

\Rightarrow Let \mathcal{G} satisfy **IndSet**. We can thus choose a set of independent vertices $S \subset V$, $|S| = k$. Let \mathcal{G}_2 be the \mathcal{G}' -subgraph induced by $S \cup A \cup B$. It is *maximal weakly label-connected* on l_2 and contains $2k + n$ edges labeled l_2 and $2k + n$ edges labeled l_1 , i.e., $\lambda(\mathcal{G}_2) = l_2$. Let \mathcal{G}_1 be the \mathcal{G}' -subgraph induced by $V \setminus S$. It is *maximal weakly label-connected* on l_1 and contains $(n+1)m$ edges, all labeled l_1 ; hence, $\lambda(\mathcal{G}_1) = l_1$. $\Phi = \{\mathcal{G}_1, \mathcal{G}_2\}$ is a valid summarization of \mathcal{G}' , as $l_1 = \max_{l \in \mathcal{G}_1}(\#l)$ and $l_2 = \max_{l \in \mathcal{G}_2}(\#l)$. \mathcal{G}' satisfies **MinSummary**.

\Leftarrow Let \mathcal{G}' satisfy **MinSummary**. We can thus compute a \mathcal{G} -partitioning, Φ , that is a *valid summarization*, where $|\Phi| \leq 2$. If $|\Phi| = 2$, then there exist two distinct \mathcal{G}' -subgraphs, $\mathcal{G}_1, \mathcal{G}_2$, where $\Phi = \{\mathcal{G}_1, \mathcal{G}_2\}$. As $\#l_1 = (n+1)m + 2k + n \geq 2n + k = \#l_2$ in \mathcal{G}' , one of the subgraphs $\mathcal{G}_1, \mathcal{G}_2$, should be such that all of its components are *maximal weakly label-connected* on l_1 . Let that subgraph be \mathcal{G}_1 . Hence, $\mathcal{G}_1 \cap \tilde{\mathcal{G}}$ contains all vertices connected by a l_1 -labeled edge. Let us denote by \tilde{V}_1 the set of vertices in $\mathcal{G}_1 \cap \tilde{\mathcal{G}}$. The set of vertices in \mathcal{G}_1 is thus $\tilde{V}_1 \cup A \cup B$. As Φ has to be a valid summarization, the set of vertices in \mathcal{G}_2 is V_2 , where $V_2 = V' \setminus (\tilde{V}_1 \cup A \cup B)$. We can thus choose the set of independent vertices of size K in \mathcal{G} to be $S = V_2$. If $|\Phi| = 1$, $\Phi = \{\mathcal{G}'\}$ must be a *valid summarization* of \mathcal{G}' . As \mathcal{G}' is *maximal weakly connected* on l_2 , it must hold that $l_2 = \max_{l \in \mathcal{G}'}(\#l)$. Hence, $K \geq 1$ and we can choose the set of independent vertices in \mathcal{G} to be $S = V' \cap V$. Thus, \mathcal{G} satisfies **IndSet**. \square

3.4 Visualizing Graph Summaries

Since a node link visualization for the GRASP summary (as shown in Figure 1 on an example) is not suitable to quickly understand the label distributions on the graph summary, we adopt a treemap visualization. This enables users to explore the graph summary, inspect the label distributions, and better comprehend the graph summary's compression factor and topology. Each cell in the treemaps of Figure 11 (depicting a 5K LDBC social network) encodes an hypernode (HN) in the graph summary. The treemaps are further enriched with links, in order to represent the underlying HEs connecting HNs. The full list of HEs, each of which is color-coded, in order to distinguish its label (as shown in the legend), is also reported. For a given HE, depending on the value of $EWeight(e, L)$, we assign a correspondingly higher/lower thickness to e (as shown for instance by thicker cyan links in Figure 11). Moreover, the links can be added or removed, by selecting and deselecting them in the legend, thus allowing to obtain different variants of Figure 11, which correspond to going from the right to the left-hand side. The linked treemaps are used to let the user better understand the graph summaries and to explain the results of the corresponding GRASP technique. In the next section, we discuss their usage during AQP and refer the reader to Section 5, for an empirical evaluation of their utility.

4 APPROXIMATE QUERY PROCESSING

4.1 Query Translations

For an input graph \mathcal{G} and a counting reachability query Q , we aim to approximate the result $\llbracket Q \rrbracket_{\mathcal{G}}$ of evaluating Q over \mathcal{G} . Hence, we translate Q into a query Q^T to be evaluated over the summarization $\hat{\mathcal{G}}$ of \mathcal{G} , such that $\llbracket Q^T \rrbracket_{\hat{\mathcal{G}}} \approx \llbracket Q \rrbracket_{\mathcal{G}}$. The translations for each input query type are given in Figure 12, using PGQL [39] as a concrete syntax. We discuss each query class next.

Simple and Optional Label (Q_L, Q_O) There are two configurations in which the label l can occur in $\hat{\mathcal{G}}$: either inside of a HN or on a cross-edge. In the first case, we cumulate the number of l -labeled HN inner-edges; in the second, we cumulate the l -labeled cross-edge weights. To account for the potential absence of l , in the optional-label query Q_2 , we additionally estimate the number of nodes in \mathcal{G}' , by cumulating the number of nodes in each HN. **Kleene Plus and Kleene Star (Q_P, Q_S)** To estimate l^+ , we cumulate the counts inside hypernodes containing l -labeled inner-edges and, as in (4.1), the weights on l -labeled cross-edges. For the first part, we use the statistics gathered during the *evaluation*

isSubclassOf isPartOf worksAt likes knows hasMember hasInterest studyAt name hasTag containerOf replyOf hasCreator hasModerator
 creationDate hasType language content locationIP browserUsed gender speaks length2 email imageFile birthday

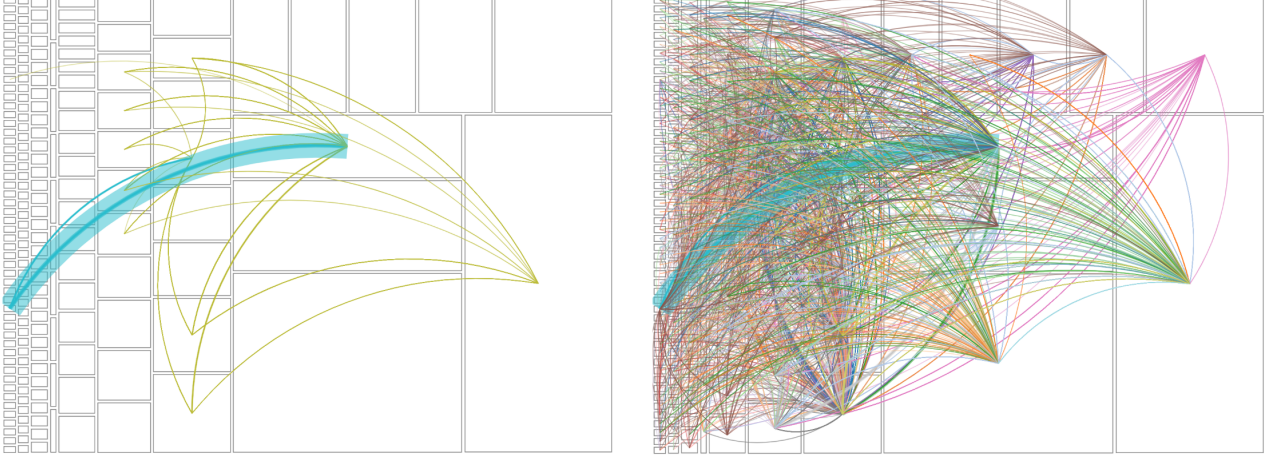


Figure 11: Coarse-grained Linked Treemap for the 5K LDBC Social Network.

phase (Sec. 3.2). We distinguish three scenarios, depending on whether the l_+ reachability is due to: 1) inner-edge connectivity – in which case we use the corresponding property counting the inner l -paths; 2) incoming cross-edges – hence, we cumulate the l -labeled in-degrees of HN vertices; or 3) outgoing cross-edges – in which case we cumulate on the number of outgoing l -paths. To handle the ϵ -label in l^* , we use the same formula as in (4.1) to additionally estimate the number of nodes in $\hat{\mathcal{G}}$.

Disjunction (Q_D) As in (4.1), we treat each configuration, considering both labels. In the first case, we cumulate the number of l_1 or l_2 -labeled HN inner-edges; in the second, we cumulate over the cross-edge weights with either label.

Binary Conjunction (Q_C) We consider all cases, depending on whether: 1) the label concatenation $l_1 \cdot l_2$ appears on a path *inside* of a HN, 2) one of the labels l_1, l_2 occurs on a HN inner-edge and the other, as a cross-edge, or 3) both labels occur on cross-edges.

Example 4.1 (Approximating Brand Reach Estimates). Revisiting Example 1.1, we evaluate the AQP-translation in Table 12 over the GRASP summary $\hat{\mathcal{G}} = (\hat{V}, \hat{E})$ in Fig. 9, as follows:

$$[Q_1]_{\hat{\mathcal{G}}} = Q_L^T(l_5) = \sum_{\hat{v} \in \hat{V}} EWeight(\hat{v}, l_5) * LPercent(\hat{v}, l_5).$$

$$\text{Hence, } [Q_1]_{\hat{\mathcal{G}}} = EWeight(HN_2, l_5) * LPercent(HN_2, l_5) = 7$$

$$[Q_2]_{\hat{\mathcal{G}}} = Q_O^T(l_2) = Q_L^T(l_2) + \sum_{\hat{v} \in \hat{V}} AvgSNVWeight(\hat{v}) * VWeight(\hat{v}).$$

$$\text{Hence, } [Q_2]_{\hat{\mathcal{G}}} = Q_L^T(l_2) = 27$$

$$[Q_3]_{\hat{\mathcal{G}}} = Q_P^T(l_0) = \sum_{\hat{v} \in \hat{V}} LReach(\hat{v}, l_0) + \sum_{\hat{e} \in \hat{E}} EWeight(\hat{e}, l_0)$$

$$\text{Hence, } [Q_3]_{\hat{\mathcal{G}}} = \sum_{\hat{v} \in \hat{V}} LReach(\hat{v}, l_0) = 15.$$

$$[Q_4]_{\hat{\mathcal{G}}} = Q_S^T(l_0) = Q_P^T(l_0) + \sum_{\hat{v} \in \hat{V}} AvgSNVWeight(\hat{v}) * VWeight(\hat{v}).$$

$$\text{Hence, } [Q_4]_{\hat{\mathcal{G}}} = 40.$$

$$[Q_5]_{\hat{\mathcal{G}}} = Q_D^T(l_4, l_1) = Q_L^T(l_4) + Q_L^T(l_1) = 14.$$

$$[Q_6]_{\hat{\mathcal{G}}} = Q_C^T(l_4, l_5) = 7.$$

Next, we will empirically study the error bounds on various datasets with queries translated according to Figure 12.

4.2 AQP and Visualization

We now discuss the utility of linked treemaps for approximate query processing. Remember from Section 3.5 that we can filter

| | |
|-----------------------------|---|
| $Q_L(l)$ | SELECT COUNT(*) MATCH () -[:l]-> () |
| $Q_L^T(l)$ | SELECT SUM(x.LPERCENT_L * x.EWEIGHT) MATCH (x) SELECT SUM(e.EWEIGHT) MATCH () -[:l]-> () |
| $Q_O(l)$ | SELECT COUNT(*) MATCH () -[:l?]-> () |
| $Q_O^T(l)$ | SELECT SUM(x.LPERCENT_L * x.EWEIGHT) MATCH (x) SELECT SUM(e.EWEIGHT) MATCH () -[:l]-> () SELECT SUM(x.AVG_SN_VWEIGHT * x.VWEIGHT) MATCH (x) |
| $Q_P(l)$ | SELECT COUNT(*) MATCH () -/:l+/-> () |
| $Q_P^T(l)$ | SELECT SUM(x.LREACH_L) MATCH (x) WHERE x.LREACH_L > 0 SELECT SUM(e.EWEIGHT) MATCH () -[:l]-> () |
| $Q_S(l)$ | SELECT COUNT(*) MATCH () -/:l+/-> () |
| $Q_S^T(l)$ | SELECT SUM(x.LREACH_L) MATCH (x) WHERE x.LREACH_L > 0 SELECT SUM(e.EWEIGHT) MATCH () -[:l]-> () SELECT SUM(x.AVG_SN_VWEIGHT * x.VWEIGHT) MATCH (x) |
| $Q_D(l_1, l_2)$ | SELECT COUNT(*) MATCH () -[:l1 l2]-> () |
| $Q_D^T(l_1, l_2)$ | SELECT SUM(x.LPERCENT_L1 * x.EWEIGHT + x.LPERCENT_L2 * x.EWEIGHT) MATCH (x) SELECT SUM(e.EWEIGHT) MATCH () -[:l1 l2]-> () |
| $Q_C(l_1, l_2, 1, 1)$ | SELECT COUNT(*) MATCH () -[:l1]-> () <[:l2]-> () |
| $Q_C(l_1, l_2, 1, 2)$ | SELECT COUNT(*) MATCH () -[:l1]-> () -[:l2]-> () |
| $Q_C(l_1, l_2, 2, 1)$ | SELECT COUNT(*) MATCH () <[:l1]-> () <[:l2]-> () |
| $Q_C(l_1, l_2, 2, 2)$ | SELECT COUNT(*) MATCH () <[:l1]-> () -[:l2]-> () |
| $Q_C^T(l_1, l_2, d_1, d_2)$ | SELECT SUM((x.RLPART_L2_L1_D2_D1 * e.EWEIGHT) / (x.LPERCENT_L1 * x.VWEIGHT)) MATCH (x) -[:l2]-> () WHERE x.LPERCENT_L1 > 0 SELECT SUM((y.RLPART_L1_L2_D1_D2 * e.EWEIGHT) / (y.LPERCENT_L2 * y.VWEIGHT)) MATCH () -[:l1]-> (y) WHERE y.LPERCENT_L2 > 0 SELECT SUM(x.EWEIGHT * min(x.LPERCENT_L1, x.LPERCENT_L2)) MATCH (x) SELECT SUM(x.EREACH_L1_L2_D1_D2) MATCH (x) |

Figure 12: Query translations onto the graph summary.

the links in the overlay, by using the checkboxes in the legend above Figure 11. This functionality lets the user understand the scope of their queries in workload and whether these are restricted to one region or to a few hypernodes and/or supernodes in the linked treemaps. Narrowing down the graph summary to only cover these queries, allows to further enhance the efficiency of approximate query evaluation, as shown in Section 5.

5 EXPERIMENTAL ANALYSIS

In this section, we present our extensive empirical evaluation recording (1) the succinctness of our GRASP summaries and the efficiency of our graph summarization algorithm; (2) the suitability of GRASP summaries for approximate evaluation of counting label-constrained reachability queries; and (3) the utility of graph visualization in driving the approximate query processing towards certain graph regions, as highlighted in the treemaps.

Setup, Datasets and Implementation. Both GRASP and the VAGQP engine are implemented in Java using OpenJDK 1.8. Note that the engine makes query calls (in PGQL) to Oracle Labs PGX 2.7, as the underlying graph database backend. Since the available version of PGX works on homogeneous graphs, rather than on heterogeneous ones, we padded each node in the graph summary with the same properties as in the other nodes. For the intermediate graph analysis operations (e.g., weakly connected components), we used Green-Marl, a domain-specific language adapted for these tasks, and modified the methods to fit with the constructions of node properties, as required by our graph summarization algorithm. Finally, the visualization overlays have been implemented using D3js. We base our analysis on four graph datasets (see Figure 13), encoding: a Bibliographic network (*bib*), the LDBC social network schema [15] (*social*), Uniprot knowledge graphs (*uniprot*), and the WatDiv schema [3] (*shop*). We obtained these using gMark [8], a synthetic graph instance and query workload generator. As gMark tries to construct the instance that best fits the given size parameter and schema constraints, we notice variations in the resulting sizes (especially for the very dense graphs *social* and *shop*). Next, on the same datasets, we generated workloads of varying sizes, for each type in Section 2, i.e., *single-label*, *Kleene-star*, *transitive closure (+)*, *unions*, and *concatenation queries*. Recent studies [10, 28] have shown that practical graph pattern queries formulated by users and in on-line query endpoints are often small: 56.5% of real-life SPARQL queries consist of a single edge (RDF triple), whereas 90.8% use 6 edges at most. Hence, we select small-sized template queries with frequently occurring topologies, such as chains [10], and formulate them on our datasets, for workloads of ~ 600 queries.

Experiments were executed on a cloud VM with Intel Xeon E312xx (4 cores) 1.80 GHz CPU, 128GB RAM, and Ubuntu 16.04.4 64-bit. Each data point was obtained by running an experiment 6 times and removing the first value from the average computation. **Compression Ratios of GRASP summaries.** First, we evaluate the effect of using the two heuristics (source-merge and target-merge) in the construction of the GRASP summaries. We measure the compression ratio *CR* obtained on the vertices and edges of the original graph (by using $(1 - |\hat{\mathcal{V}}|/|\mathcal{V}|) * 100$ and $(1 - |\hat{\mathcal{E}}|/|\mathcal{E}|) * 100$, respectively for the CR vertices and edges), along with the *summary construction time* (SCT). Recall that our graph summaries are encoded using the property graph data model and, as such, they possess node and edge properties.

Next, we discuss the results for source merge and then compare them with those for target merge. In Figures 14 (a) and (b), we can observe that the most homogeneous datasets, (*bib*) and (*uniprot*), achieve very high CR (close to 100%) and steadily maintain it with varying graph sizes. As far as heterogeneity significantly grows for (*shop*) and (*social*), the CR becomes eagerly sensitive to the dataset size, starting with low values, for smaller graphs, and achieving a plateau between 85% and 90%, for larger ones. Consequently, our GRASP algorithm enables us to obtain compact summaries for large, highly heterogeneous

datasets. Notice also that the most heterogeneous datasets, (*shop*) and (*social*), although close to each other, display a symmetric behavior for the CRs of vertices and edges: the former better compresses vertices, while the latter, edges. Concerning the SCT runtime in Figure 14 (c), all datasets keep a reasonable performance for larger sizes, including the most heterogeneous one (*shop*). The runtime is, in fact, not affected by the heterogeneity degree, but is rather sensitive, for larger sizes, to variations in $|E|$ (up to 450K and 773K, for *uniprot* and *social*).

We now contrast the source-merge (s-m) and target-merge (t-m) heuristics, the latter being reported in Figure 14 (d-e-f). We observe that, while the SCT runtime is quite similar for the two, target-merge achieves better CRs for the social network dataset. Overall, the dataset with the worst CR across the two heuristics is *shop*, which has the lowest CR for smaller sizes. This is also due to the high number of labels in the initial *shop* instances, and hence, to the high number of properties needed for its summary, compared to the other tested datasets: on average, across all considered sizes, its summary requires 62.33 properties, against 17.67 for the social graph one, 10.0, for *bib*, and 14.0, for *uniprot*. Nevertheless, even for *shop* and especially for large sizes, the CRs are fairly high. These experiments show that, despite its high complexity, GRASP provides high CRs and low SCT runtimes.

AQP Accuracy on GRASP summaries. We measured the *accuracy* and *efficiency* of our VAGQP engine by using the *relative error* and, respectively, the *time gain* measures. The relative error (per query Q_i) is: $1 - \min(Q_i(\mathcal{G}), Q_i^T(\hat{\mathcal{G}})) / \max(Q_i(\mathcal{G}), Q_i^T(\hat{\mathcal{G}}))$ (in %), where $Q_i(\mathcal{G})$ is the result of the counting query Q_i on the original graph (executed with PGX) and $Q_i^T(\hat{\mathcal{G}})$, that of the translated query Q_i^T on the GRASP summary (executed with our engine). The time gain is: $t_{\mathcal{G}} - t_{\hat{\mathcal{G}}} / \max(t_{\mathcal{G}}, t_{\hat{\mathcal{G}}})$ (in %), where the times $t_{\mathcal{G}}$ and $t_{\hat{\mathcal{G}}}$ are the query evaluation times of query Q_i on the original graph and on the GRASP summary, respectively.

For the Disjunction, Kleene-plus, Kleene-star, Optional and Single Label query types, we have generated workloads of different sizes, bound by the number of labels in each dataset. For the concatenation workloads, we considered binary conjunctive queries without disjunction, recursion, or optionality. Note that, currently, GRASP summaries do not support compositionality.

Figure 15 (a) and (b) show the relative error and the average time gain for Disjunction, Kleene-plus, Kleene-star, Optional and Single Label workloads. In Figure 15 (a), we can observe that the avg relative error is kept low in all cases and is bounded by 5.5% in the case of social dataset’s Kleene-plus and Kleene-star workloads. In all the other cases, including Kleene-plus and Kleene-star workloads for *shop* dataset, the error is relatively small and near to 0%. This experiment confirms the effectiveness of our GRASP summaries for approximate evaluation of graph queries. In Figure 15 (b), we studied the efficiency of AQP on GRASP summaries by reporting the time gain (in %) compared with the query evaluation on the original graphs for the four datasets. We can notice a positive time gain (greater or equal to 75%) in most cases, but for disjunction. Although the AQP relative error is still advantageous for disjunction, disjunctive queries are time-consuming for AQP on GRASP summaries and can take very long for extremely heterogeneous datasets, such as *shop* (which have the most labels). We believe that the performance of these queries will improve with the next PGX version.

Figures 17 (a) and (b) show the comparison among the most heterogeneous datasets (*shop* and *social*) on workloads of binary conjunctive queries (on a total of 14 queries, 7 per dataset). We

| Dataset | $ L_V $ | $ L_E $ | ~ 1K | | ~ 5K | | ~ 25K | | ~ 50K | | ~ 100K | | ~ 200K | |
|----------------|---------|---------|-------|-------|-------|-------|-------|-------|-------|--------|--------|--------|--------|--------|
| | | | $ V $ | $ E $ | $ V $ | $ E $ | $ V $ | $ E $ | $ V $ | $ E $ | $ V $ | $ E $ | $ V $ | $ E $ |
| <i>bib</i> | 5 | 4 | 916 | 1304 | 4565 | 6140 | 22780 | 3159 | 44658 | 60300 | 88879 | 119575 | 179356 | 240052 |
| <i>social</i> | 15 | 27 | 897 | 2127 | 4434 | 10896 | 22252 | 55760 | 44390 | 110665 | 88715 | 223376 | 177301 | 450087 |
| <i>uniprot</i> | 5 | 7 | 2170 | 3898 | 6837 | 18899 | 25800 | 97059 | 47874 | 192574 | 91600 | 386810 | 177799 | 773082 |
| <i>shop</i> | 24 | 82 | 3136 | 4318 | 6605 | 10811 | 17893 | 34052 | 31181 | 56443 | 57131 | 93780 | 109205 | 168934 |

Figure 13: gMark-Generated Dataset Characteristics: number of vertices $|V|$, edges $|E|$, vertex $|L_V|$ and edge labels $|L_E|$.

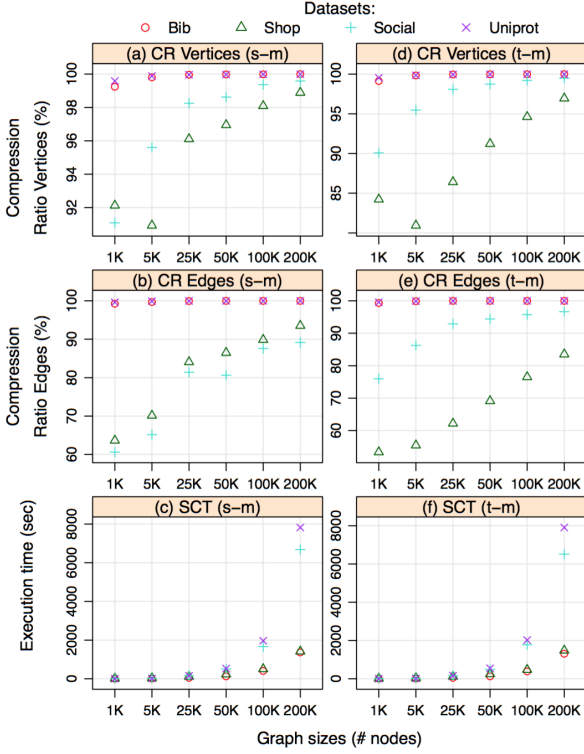


Figure 14: Compression Ratios for vertices and edges along with SCT runtime for various sizes of graph datasets for both source-merge (a) to (c) and target-merge (d) to (f).

report the relative error and time gain per query instead of per workload, as before. We can observe in Figure 17 (a) a relatively small error for almost all queries (with an average of 1.6%), and an upper bound of 8.44% for query Q5. Finally, the shop dataset exhibits a relatively small error with an average of 0.14%.

Figure 17 (b) illustrates the fairly high VAGQP time gains for conjunctive queries. Prominently, for the social and shop datasets, VAGQP is 81.64% and 70.95% faster than query evaluation on the original graph. This dataset difference is due to the large number of properties and to the high heterogeneity of the latter.

Baseline for GRASP-based AQP performance. The closest system to ours is SumRDF [34] (see Section 6), which, however, operates on a *simpler edge-labeled model rather than on property graphs and is tailored for estimating the results of conjunctive queries only*. To set a baseline for GRASP-based AQP, we considered the shop dataset in gMark [8], simulating the WatDiv benchmark [3] (also adopted as a benchmark in the SumRDF paper [34]). From this dataset with 31K nodes and 56K edges, we generated the corresponding SumRDF and GRASP summaries. We noted that GRASP registers a better CR ratio than SumRDF, with 2737 nodes vs. 3480 resources and 17430 edges vs. 29621 triples. This comparison is, however, tentative, as GRASP compresses vertices

independently of the edges, while SumRDF returns triples. We then considered the same type of conjunctive queries analyzed in Figure 17 and whose syntax is reported in Figure 16. Comparing GRASP vs. SumRDF (see Figure 16), we recorded an *average relative error* of estimation of only 0.15% vs. 2.5% and an *average query runtime* of only 27.55 ms vs. 427.53 ms. The superior accuracy and time performance of GRASP-based AQP show the promise of our approach, motivating our aim to scale towards a fully compositional solution. As SumRDF does not support disjunctions, Kleene-star/plus queries and optional queries, further comparisons were not feasible.

Treemap Utility for AQP on GRASP summaries. Treemaps allow users to analyze the topology of a GRASP summary, \hat{G} , to explore and to navigate its label distribution. Next, we highlight a possible use of treemaps to improve query evaluation runtime. Given the translation of a conjunctive query, $Q_C^T(l_1, l_2, d_1, d_2)$, the coarse-grained view can reveal if the labels l_1 or l_2 are located in a particular region of \hat{G} , as in Figure 11 (b), where both labels are concentrated in the left region of the GRASP summary (each color representing a different label). This information can be useful to filter out the graph summary regions that are not inspected by the queries. As a test-case for this treemap usage, we have considered queries in the first workload (e.g., single label, disjunction, Kleene star, etc.) and showed the runtime improvement the coarse-grained treemap refinement. We have observed a non-negligible improvement in all datasets, i.e. 35.73% for shop, 27.24% for social, 27.56% for uniprot and 27.15% for bib.

6 RELATED WORK

Chaudhuri et al. highlighted in [12] the two-fold importance of AQP in the world of Big Data: (i) to give users agency in deciding the accuracy vs. efficiency trade-off and (ii) to ensure query-independent accuracy guarantees. Our work leverages both points, as it targets approximate graph query processing and it illustrates how the blend between AQP and graph data visualization enables advanced graph analytics.

Previous influential work on AQP has focused on relational languages (SQL and restricted OLAP queries), by embedding samplers directly in the query language and evaluating them in the query plan [1, 12]. Relational rows are sampled uniformly-at-random with a given probability. Uniform sampling is widely supported by AQP performing RDBMSs, by Big Data systems, e.g., Spark SQL, Oracle, Microsoft’s Power BI, SnappyData, Google’s BigQuery, and by online aggregation methods [21, 23]. Different classes of samplers exist, ranging from the less accurate, uniform ones, to the distinct and universe ones that work on small groups and, respectively, on join operators in the query plans.

Preliminary work on approximate graph analytics in a distributed setting has recently been pursued in [22]. They rather focus on a graph sparsification technique and small samples, in order to approximate the results of specific graph algorithms, such as PageRank and triangle counting on undirected graphs. In contrast, our approach operates in a centralized setting and relies

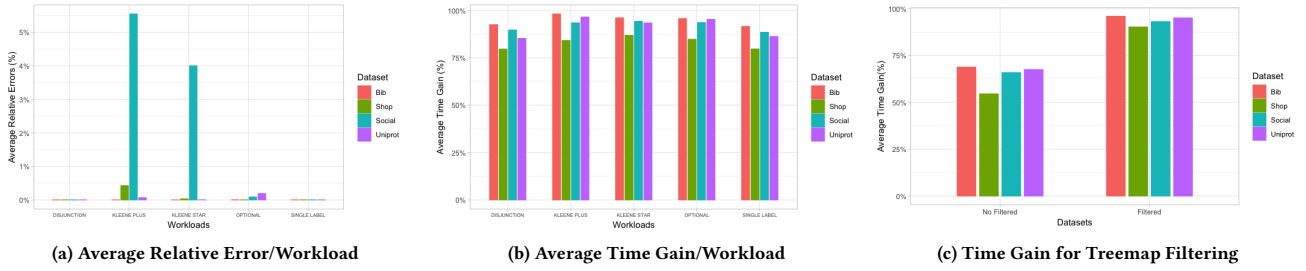


Figure 15: Relative Error (a) and Time Gain (b) per Workload, in each Dataset, for 200K nodes and Single Label, Disjunction, Kleene Star/Plus and Optional Queries, Time Gain (c) for Filtering Coarse-Grained Treemap.

| ID | Query | Estimated Answer | | Relative Error (%) | | Runtime (ms) | |
|----|--|------------------|-------|--------------------|-------|--------------|-------|
| | | SumRDF | GRASP | SumRDF | GRASP | SumRDF | GRASP |
| Q1 | SELECT COUNT(*) MATCH (x0)-[:producer]->()<[:paymentAccepted]-(x1) | 75 | 76 | 1.32 | 0.00 | 136.30 | 38.2 |
| Q2 | SELECT COUNT(*) MATCH (x0)-[:totalVotes]->()<[:price]-(x1) | 42.4 | 44 | 3.64 | 0.00 | 50.99 | 17 |
| Q3 | SELECT COUNT(*) MATCH (x0)-[:jobTitle]->()<[:keywords]-(x1) | 226.7 | 221 | 2.51 | 0.18 | 463.85 | 12.8 |
| Q4 | SELECT COUNT(*) MATCH (x0)-[:title]->()<[:performedIn]-(x1) | 19.5 | 20 | 2.50 | 0.00 | 831.72 | 8.8 |
| Q5 | SELECT COUNT(*) MATCH (x0)-[:artist]->()<[:employee]-(x1) | 143.3 | 133 | 7.19 | 0.37 | 196.77 | 10.6 |
| Q6 | SELECT COUNT(*) MATCH (x0)-[:follows]->()<[:editor]-(x1) | 524 | 528 | 0.38 | 0.48 | 1295.83 | 19 |

Figure 16: SumRDF and GRASP performance: approximate evaluation of binary conjunctive queries on the respective summaries of a shop graph instance with 31K nodes and 56K edges; comparing estimated cardinality (number of computed answers), relative error w.r.t results computed on the original graph, and query runtime.

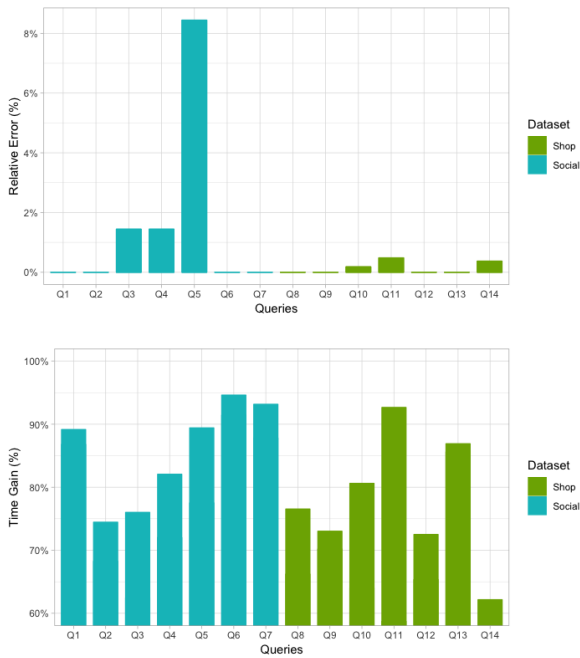


Figure 17: Relative Error (top) and Time Gain (bottom), per Conjunctive Query, in each Dataset, for 50K nodes.

on query-driven graph summarization for graph navigational queries with aggregates, while interleaving it with information visualization techniques devoted to orientate AQP evaluation towards the regions of the graph pertinent to the queries.

RDF graph summarization for cardinality estimation has been tackled in recent work [34]. Their main goal is RDF query cardinality estimation and on a data model that is less expressive

than ours (plain RDF graphs vs. property graphs). Hence, the query fragments considered in our and in theirs have limited overlap. As reported in Section 5, our approximate evaluation shows better accuracy and runtime on a set of common queries.

An algorithm for answering graph reachability queries, using graph simulation based pattern matching, is given in [16, 17], to construct query preserving summaries. This work differs from ours, as it does not consider property graphs or aggregates.

Aggregation-based graph summarization [25] is at the heart of previous approaches, the most notable of which is SNAP [37]. However, SNAP and its successor, k-SNAP [43], are not suitable for AQP and are mainly devoted to discovery-driven graph summarization of heterogeneous networks by relying on a notion of interestingness. These approaches pioneer user interaction as a mean to control the resolutions of the graph summary. However, user intervention here is basically used to drill-down or roll-up to navigate through summaries with different resolutions. More recently, preliminary work by Rudolf et al. [32] has introduced a graph summary suitable for property graphs based on a set of input summarization rules. In the spirit of SNAP, their summary is conceived for the property graph cube and supports OLAP operations of the kind roll-up, drill-down and slice dice for reducing/expanding the cube dimensions. They further tackle the problems of unbalanced hierarchies and OLAP anomalies. They do not support label-constrained reachability queries and VGAQP as we do in this paper. In [36], a graphical sketch for summarizing graph streams is introduced. While it supports dynamic graphs and provides constant maintenance time per update, the summary stores no extra information and is not used for AQP.

Visualization has recently been pinpointed as a fertile ground for data management⁴, in the context of the too-many-tuples and too-many-visualization problems. In our paper, we focus on

⁴ACM Sigmod Blog hosts Aditya Parameswaran, 2018

the graph DBMS case, in which these problems are further exacerbated by the fact that interlinking structures must be preserved in the evaluation of graph navigational queries. Optimistic visualization is introduced in the PanGloss system [29], in order to let the user quickly retrieve AQP results, by only considering a few relational tuples, and to keep him/her busy until new ones arrive. Contrary to PanGloss, we do not consider the human-interaction aspect of VAGQP, which deserves further attention in our future work. Graph summaries applied to answer subgraphs, returned by formulating keyword queries on large networks, are used in order to enhance the user’s understandability of query results in [41]. Our query classes are significantly different from theirs.

The IDEA system [19] leverages other visualization overlays, i.e., heat-maps, where each cell represents the relationship count between two attributes in a relation. They focus on the rare subpopulation case and on the construction of suitable indexes.

The AQP++ system [30] blends AQP with aggregate precomputation, such as data cubes, to handle aggregate relational queries. This unified approach performs better, in terms of preprocessing, runtime, and quality, than plain AQP.

7 CONCLUSION AND PERSPECTIVES

This paper presents the GRASP graph summarization technique, suitable for label-constrained counting reachability queries on property graphs. We prove that the problem of deciding whether an optimal graph summary exists, i.e., such that the number of label-constrained graph partitions is minimal, is NP-complete. We then leverage our GRASP summaries and their linked treemap encoding for AQP purposes. The experiments ran on various datasets show both fairly high compression ratios, for the summaries, and low relative error and time gain, for the AQP. We also illustrate the advantages of using linked treemaps as summary encoding, for both human-explainability and AQP refinement. As future work, we aim to further explore the interplay between visualization techniques and AQP and to support more graph analytics and aggregation operators. As our approach is system-agnostic, being applicable to any framework supporting the property graph model and the query fragment in Fig. 4, we would like to implement it on top of other graph query engines in the near future. Furthermore, we plan to make open-source the VAGQP prototype and its visualization plug-in.

REFERENCES

- [1] S. Acharya, P. B. Gibbons, and V. Poosala. Congressional Samples for Approximate Answering of Group-by Queries. In *SIGMOD*, pages 487–498, 2000.
- [2] S. Agarwal, B. Mozafari, A. Panda, H. Milner, S. Madden, and I. Stoica. Blinkdb: queries with bounded errors and bounded response times on very large data. In *EuroSys*, pages 29–42, 2013.
- [3] G. Aluç, O. Hartig, M. T. Özsu, and K. Daudjee. Diversified stress testing of RDF data management systems. In *ISWC*, pages 197–212, 2014.
- [4] R. Angles. The property graph database model. In *AMW*, 2018.
- [5] R. Angles, M. Arenas, P. Barceló, P. A. Boncz, G. H. L. Fletcher, C. Gutierrez, T. Lindaaker, M. Paradies, S. Plantikow, J. F. Sequeda, O. van Rest, and H. Voigt. G-CORE: A core for future graph query languages. In *SIGMOD*, pages 1421–1432, 2018.
- [6] R. Angles, M. Arenas, P. Barceló, A. Hogan, J. L. Reutter, and D. Vrgoc. Foundations of modern query languages for graph databases. *ACM Comput. Surv.*, 50(5):68:1–68:40, 2017.
- [7] A. Aris and B. Shneiderman. Designing semantic substrates for visual network exploration. *Information Visualization*, 6(4):281–300, 2007.
- [8] G. Bagan, A. Bonifati, R. Ciucanu, G. H. L. Fletcher, A. Lemay, and N. Advokaat. gmark: Schema-driven generation of graphs and queries. *IEEE Trans. Knowl. Data Eng.*, 29(4):856–869, 2017.
- [9] A. Bonifati, G. Fletcher, H. Voigt, and N. Yakovets. *Querying Graphs*. Synthesis Lectures on Data Management. Morgan & Claypool Publishers, 2018.
- [10] A. Bonifati, W. Martens, and T. Timm. An analytical study of large SPARQL query logs. *PVLDB*, 11(2):149–161, 2017.
- [11] D. Calvanese, G. De Giacomo, M. Lenzerini, and M. Y. Vardi. Rewriting of regular expressions and regular path queries. *J. Comput. Syst. Sci.*, 64(3):443–465, 2002.
- [12] S. Chaudhuri, B. Ding, and S. Kandula. Approximate Query Processing: No Silver Bullet. In *SIGMOD*, pages 511–519, 2017.
- [13] M. P. Consens and A. O. Mendelzon. GraphLog: a Visual Formalism for Real Life Recursion. *PODS*, pages 404–416, 1990.
- [14] I. F. Cruz, A. O. Mendelzon, and P. T. Wood. A graphical query language supporting recursion. In *SIGMOD*, pages 323–330, 1987.
- [15] O. Erling, A. Averbuch, J. Larriba-Pey, H. Chafi, A. Gubichev, A. Prat-Pérez, M. Pham, and P. A. Boncz. The LDDB Social Network Benchmark: Interactive Workload. In *SIGMOD*, pages 619–630, 2015.
- [16] W. Fan, J. Li, S. Ma, N. Tang, and Y. Wu. Adding regular expressions to graph reachability and pattern queries. In *ICDE*, pages 39–50, 2011.
- [17] W. Fan, J. Li, X. Wang, and Y. Wu. Query preserving graph compression. In *SIGMOD*, pages 157–168, 2012.
- [18] I. F. Fekete, D. Wang, N. Dang, and C. Plaisant. Overlaying Graph Links on Treemaps. In *Information Visualization*, 2003.
- [19] A. Galakatos, A. Crotty, E. Zraggen, C. Binnig, and T. Kraska. Revisiting reuse for approximate query processing. *PVLDB*, 10(10):1142–1153, 2017.
- [20] M. R. Garey and D. S. Johnson. *Computers and Intractability: A Guide to the Theory of NP-Completeness*. W. H. Freeman, 1979.
- [21] J. M. Hellerstein, P. J. Haas, and H. J. Wang. Online aggregation. In *SIGMOD*, pages 171–182, 1997.
- [22] A. P. Iyer, A. Panda, S. Venkataraman, M. Chowdhury, A. Akella, S. Shenker, and I. Stoica. Bridging the GAP: towards approximate graph analytics. In *GRADES*, pages 10:1–10:5, 2018.
- [23] C. Jermaine, S. Arumugam, A. Pol, and A. Dobra. Scalable approximate query processing with the dbo engine. *ACM Trans. Database Syst.*, 33(4), 2008.
- [24] R. Jin, H. Hong, H. Wang, N. Ruan, and Y. Xiang. Computing label-constraint reachability in graph databases. In *SIGMOD*, pages 123–134, 2010.
- [25] A. Khan, S. S. Bhowmick, and F. Bonchi. Summarizing static and dynamic big graphs. *PVLDB*, 10(12):1981–1984, 2017.
- [26] A. Khandelwal, Z. Yang, E. Ye, R. Agarwal, and I. Stoica. Zipq: A memory-efficient graph store for interactive queries. In *SIGMOD*, pages 1149–1164, 2017.
- [27] Y. Liu, A. Dighe, T. Safavi, and D. Koutra. Graph summarization methods and applications: A survey. *CoRR*, abs/1612.04883, 2016.
- [28] S. Malyshev, M. Krotzsch, L. Gonzalez, J. Gonsior, and A. Bielefeldt. Getting the most out of wikidata: Semantic technology usage in wikipedia’s knowledge graph. In *ISWC (to appear)*. LNCS, 2018.
- [29] D. Moritz, D. Fisher, B. Ding, and C. Wang. Trust, but verify: Optimistic visualizations of approximate queries for exploring big data. In *CHI*, pages 2904–2915, 2017.
- [30] J. Peng, D. Zhang, J. Wang, and J. Pei. AQP++: connecting approximate query processing with aggregate precomputation for interactive analytics. In *SIGMOD*, pages 1477–1492, 2018.
- [31] J. A. L. Poutre and J. van Leeuwen. Maintenance of Transitive Closures and Transitive Reductions of Graphs. In *WG*, pages 106–120, 1987.
- [32] M. Rudolf, H. Voigt, C. Bornhövd, and W. Lehner. Synopsys: Foundations for multidimensional graph analytics. In *BIRTE*, pages 159–166, 2014.
- [33] S. Sahu, A. Mhedhbi, S. Salihoglu, J. Lin, and M. T. Özsu. The ubiquity of large graphs and surprising challenges of graph processing. *PVLDB*, 11(4):420–431, 2017.
- [34] G. Stefanoni, B. Motik, and E. V. Kostylev. Estimating the cardinality of conjunctive queries over rdf data using graph summarisation. In *WWW*, pages 1043–1052, 2018.
- [35] G. Szárnyas, A. Prat-Pérez, A. Averbuch, J. Marton, M. Paradies, M. Kaufmann, O. Erling, P. A. Boncz, V. Haprian, and J. B. Antal. An early look at the LDDB social network benchmark’s business intelligence workload. In *GRADES*, pages 9:1–9:11, 2018.
- [36] N. Tang, Q. Chen, and P. Mitra. Graph stream summarization: From big bang to big crunch. In *SIGMOD*, pages 1481–1496, 2016.
- [37] Y. Tian, R. A. Hankins, and J. M. Patel. Efficient aggregation for graph summarization. In *SIGMOD*, pages 567–580. ACM, 2008.
- [38] L. G. Valiant. The complexity of enumeration and reliability problems. *SIAM J. Comput.*, 8(3):410–421, 1979.
- [39] O. van Rest, S. Hong, J. Kim, X. Meng, and H. Chafi. PGQL: a property graph query language. In *GRADES*, page 7, 2016.
- [40] P. T. Wood. Query languages for graph databases. *SIGMOD Record*, 41(1):50–60, 2012.
- [41] Y. Wu, S. Yang, M. Srivatsa, A. Iyengar, and X. Yan. Summarizing answer graphs induced by keyword queries. *PVLDB*, 6(14):1774–1785, 2013.
- [42] K. Zeng, S. Agarwal, A. Dave, M. Armbrust, and I. Stoica. G-OLA: generalized on-line aggregation for interactive analysis on big data. In *SIGMOD*, pages 913–918, 2015.
- [43] N. Zhang, Y. Tian, and J. M. Patel. Discovery-driven graph summarization. In *ICDE*, pages 880–891. IEEE Computer Society, 2010.